REDVET - Revista electrónica de Veterinaria - ISSN 1695-7504
Vol 25, No.2 (2024)
http://www.veterinaria.org
Received: Revised: Accepted:

Structural, Electrical, and Optoelectronic Investigation of $Cs_3Bi_2I_9$ Perovskite

Hiral Patel[1*], Piyush Vyas[2]

[1*]Chemistry Department, Amity University, Gwalior-474005, Madhya Pradesh, India,
E-mail: hiralpatela16@gmail.com
[2]Chemistry Division, Sheth M. N. Science College, Patan-384265, Gujarat, India

ABSTRACT
TC$s_3Bi_2I_9$ is a lead-free halide perovskite with promising stability and optoelectronic properties. In this work, it was synthesized and systematically studied through structural, DC electrical, impedance, and photodetection measurements. Structural analysis confirms the formation of a well-crystalline phase with good phase purity. DC conductivity shows thermally activated behavior, indicating semiconducting nature. Complex impedance results reveal grain and grain-boundary contributions, with decreasing resistance at higher temperatures. The material also exhibits a clear photoresponse with enhanced photocurrent under illumination. Overall, $Cs_3Bi_2I_9$ demonstrates good electrical and optoelectronic performance, making it suitable for semiconductor and photodetector applications.

Keywords: $Cs_3Bi_2I_9$, lead-free perovskite, DC electrical conductivity, complex impedance spectroscopy, photodetector, optoelectronic properties.

Introduction

In recent years, lead-based halide perovskites have attracted significant attention due to their exceptional optoelectronic properties, including high absorption coefficients, long carrier diffusion lengths, and tunable bandgaps. These characteristics have enabled remarkable progress in photovoltaic devices, photodetectors, light-emitting diodes, and other optoelectronic applications. However, the inherent toxicity of lead and the associated environmental and stability concerns have motivated the search for lead-free alternatives.1-5

Among the emerging lead-free perovskite candidates, bismuth-based compounds have gained considerable interest due to the chemical stability and low toxicity of Bi^{3+}, which is isoelectronic with Pb^{2+} in certain configurations.6,7 In particular, $Cs_3Bi_2I_9$ has emerged as a promising material owing to its improved air stability, non-toxic nature, and unique low-dimensional crystal structure. Unlike the three-dimensional framework of conventional ABX_3 perovskites, $Cs_3Bi_2I_9$ typically crystallizes in a zero-dimensional (0D) or layered structure composed of isolated $Bi_2I_9^{3-}$ bioctahedral units separated by Cs^+ ions. This structural arrangement strongly influences its electronic and optical behavior.8-10

The structural properties of $Cs_3Bi_2I_9$ play a crucial role in determining its electronic band structure, defect tolerance, and charge transport characteristics. The material generally exhibits a wide bandgap in the range of ~2.0-2.3 eV, which limits its efficiency in single-junction solar cells but makes it suitable for UV photodetectors and high-energy photon harvesting applications. Understanding its crystallographic phase, lattice dynamics, and defect states is essential for optimizing its performance in device applications.11

From an electrical perspective, $Cs_3Bi_2I_9$ is known to exhibit relatively low electrical conductivity and short carrier diffusion lengths due to its low-dimensional structure and strong electron–phonon coupling. These factors contribute to significant carrier localization and recombination, which directly impact device efficiency. Various strategies such as doping, compositional engineering, and nanostructuring have been explored to improve its charge transport properties.12-14

Optoelectronic investigations of $Cs_3Bi_2I_9$ reveal strong light–matter interactions, including pronounced excitonic effects and absorption in the visible region. The material has demonstrated potential in photodetection and radiation sensing applications due to its stability and relatively high absorption coefficient. However, further understanding of its recombination mechanisms, trap states, and exciton binding energy is required to fully exploit its optoelectronic capabilities.15-17

In this work, we present a comprehensive study of the structural, electrical, and optoelectronic properties of $Cs_3Bi_2I_9$ perovskite. By correlating crystallographic features with charge transport and optical behavior, this investigation aims to provide deeper insight into the fundamental properties of $Cs_3Bi_2I_9$ and its potential for next-generation lead-free optoelectronic devices.

Experimental

The synthesis of CsPbI3 was carried out via a solution-based method, ensuring phase purity. Structural analysis was performed using XRD, followed by morphological characterization via FESEM. Elemental composition was verified using ED-XRF spectroscopy. Optical properties were studied using UV-Vis spectroscopy and photoluminescence (PL) measurements. Dielectric behavior was analyzed through impedance spectroscopy across different temperatures and frequencies. Finally, the optoelectronic properties were evaluated using a two-probe method under varying light intensities.

REDVET - Revista electrónica de Veterinaria - ISSN 1695-7504
Vol 25, No.2 (2024)
http://www.veterinaria.org
Received: Revised: Accepted:

Synthesis of Cesium bismuth iodide ($Cs_3Bi_2I_9$)

$Cs_3Bi_2I_9$ was synthesized via a simple wet chemical method under ambient conditions. All glassware was cleaned with deionized water and rinsed with absolute alcohol prior to use. Initially, 3 mM (779.43 mg) of CsI was dissolved in 30 mL of DMF under constant stirring for 2 h at room temperature to form a homogeneous solution. Subsequently, 2 mM (897.42 mg) of BiI_3 was added and stirred vigorously for 2 h at 60 °C to ensure complete reaction. Isopropyl alcohol (IPA) was then added dropwise to induce precipitation of $Cs_3Bi_2I_9$. The resulting product was filtered, washed several times with ethanol, and dried under vacuum overnight. The obtained powder was used for further characterization.

Results And Discussin

For perovskite materials, even slight changes in structural composition can lead to significant variations in their physical properties. The crystalline structure of as-synthesized $Cs_3Bi_2I_9$ was investigated using powder X-ray diffraction (XRD) at room temperature under ambient conditions. It is well known that many inorganic–organic hybrid perovskites degrade rapidly in the presence of moisture; however, in this study, electrochemical measurements were carried out using an aqueous Na_2SO_4 electrolyte. Therefore, the stability of $Cs_3Bi_2I_9$ in an aqueous environment was critically examined.

XRD patterns were recorded for both the as-synthesized sample and the water-treated sample in the 2θ range of 10°–60°. No significant shift in peak positions was observed after water treatment, confirming the excellent structural stability of $Cs_3Bi_2I_9$ in aqueous conditions (Figure 1a). The diffraction peaks at 12.04°, 12.71°, 25.16°, 25.83°, 27.44°, 29.88°, and 43.10° correspond to the (100), (101), (006), (202), (203), (204), and (220) planes, respectively, indicating a hexagonal crystal structure with a primitive cell and $P6_3/mnc$ space group. Field emission scanning electron microscopy (FESEM) revealed an agglomerated morphology composed of densely packed granular structures with sizes ranging from 200-300 nm. The porous nature of the surface provides a large number of active sites, which is beneficial for electrochemical interactions (Figure 1b).

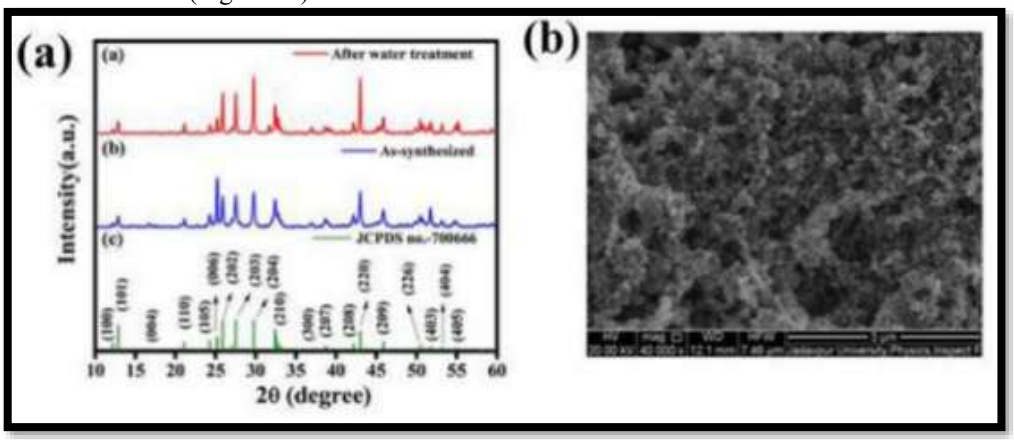

Figure 1: (a) X-ray diffraction spectra of $Cs_3Bi_2I_9$; (b) FESEM image of $Cs_3Bi_2I_9$.

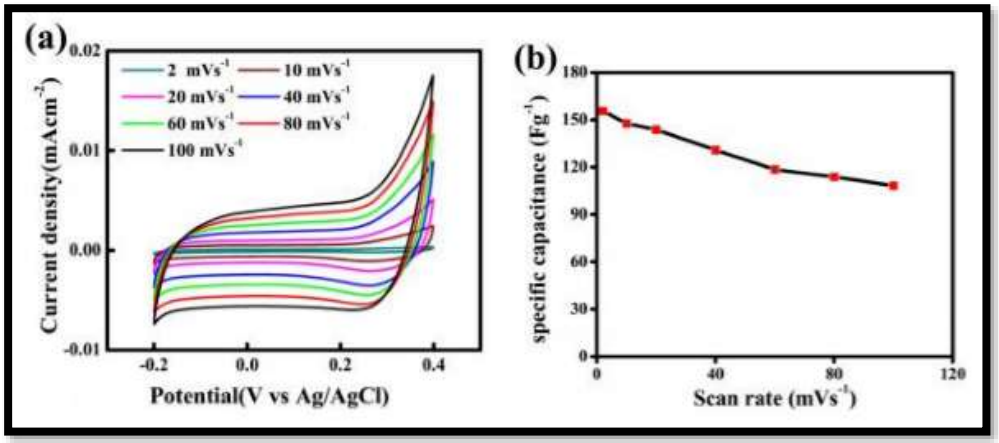

Figure 2: (a) CV profile in 3-electro demeasurement for different scanrate of $Cs_3Bi_2I_9$; (b) Scanrate dependent specific capacitance of $Cs_3Bi_2I_9$.

Figure 2(a) shows the cyclic voltammetry (CV) curves of $Cs_3Bi_2I_9$ recorded at scan rates ranging from 2 to 100 mV s^{-1} in Na_2SO_4 aqueous electrolyte. The quasi-rectangular shape with slight distortion indicates combined electric double-layer capacitance and pseudocapacitive behavior. The increase in current density with scan rate, while maintaining the

REDVET - Revista electrónica de Veterinaria - ISSN 1695-7504
Vol 25, No.2 (2024)
http://www.veterinaria.org
Received: Revised: Accepted:

curve shape, suggests good electrochemical reversibility and efficient ion transport. The absence of distinct redox peaks confirms predominantly surface-controlled capacitive processes. Figure 2(b) presents the variation of specific capacitance with scan rate. The capacitance decreases with increasing scan rate due to limited ion diffusion at higher scan rates, which restricts electrolyte access to inner active sites. At lower scan rates, improved ion penetration leads to higher utilization of active sites and enhanced capacitance, confirming good rate capability of $Cs_3Bi_2I_9$.

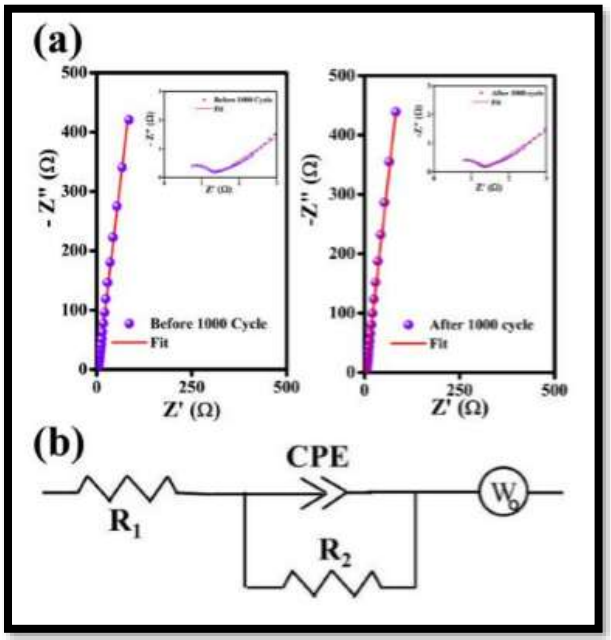

Figure 3: (a) Nyquist plot of Cs3Bi2I9 in a frequency range.01Hz-106Hz,((b) equivalentcircuit.

Figure 3 (a) shows the Nyquist plots of $Cs_3Bi_2I_9$ recorded before and after 1000 charge-discharge cycles in the frequency range of 0.01 Hz-10^6 Hz. The nearly vertical line in the low-frequency region indicates dominant capacitive behavior and efficient ion diffusion. The similarity of the Nyquist plots before and after cycling suggests excellent electrochemical stability and good charge-transfer characteristics of the electrode material. The inset highlights the high-frequency region, where a small semicircle corresponds to the charge-transfer resistance. Figure 3 (b) presents the equivalent electrical circuit used to fit the impedance data, consisting of a solution resistance (R_1), a charge-transfer resistance (R_2), and a constant phase element (CPE). The good agreement between the experimental and fitted curves confirms the reliability of the proposed circuit model and the stable electrochemical performance of $Cs_3Bi_2I_9$. Data shown in Table 1.

Table 1.The value of equivalent circuitelement

Component	Value	
	Before1000cycle	After1000cycle
R1(Ω)	0.09	0.061
CPE-T	2.76x10-5	2.68x10-5
CPE-P	0.758	0.746
R2(Ω)	1.2	1.2
W1-R	7.388	8.535
W1-T	0.164	0.186
W1-P	0.441	0.443

Conclusion

In summary, lead-free $Cs_3Bi_2I_9$ perovskite was successfully synthesized by a simple wet chemical method and its structural, electrical, and optoelectronic properties were systematically investigated. X-ray diffraction analysis confirmed the formation of a highly crystalline and phase-pure hexagonal structure, while morphological studies revealed a porous and agglomerated nanostructure. DC conductivity measurements demonstrated thermally activated semiconducting be havior, indicating enhanced charge transport at elevated temperatures. Impedance spectroscopy revealed significant contributions from both grain and grain-boundary effects, with a decrease in resistance upon increasing temperature, confirming the thermally activated conduction mechanism. Furthermore, the material exhibited a pronounced photoresponse with enhanced photocurrent under illumination, highlighting its excellent light-harvesting capability. These findings demonstrate that $Cs_3Bi_2I_9$ possesses good structural stability, favorable electrical characteristics, and promising optoelectronic performance, making it a potential candidate for future semiconductor and photodetector applications.

REDVET - Revista electrónica de Veterinaria - ISSN 1695-7504
Vol 25, No.2 (2024)
http://www.veterinaria.org
Received: Revised: Accepted:

Funding
No funding received for this work.

Acknowledgment
The authors express their gratitude to the Department of Chemistry Sheth M. N. Science College, Patan, and Department of Chemistry Amity University, Gwalior for their assistance with experimental work and analysis support.

References

1. Hamukwaya, S. L., Hao, H., Mashingaidze, M. M., Zhong, T., Tang, S., Dong, J., ... & Liu, H. (2022). Potassium iodide-modified lead-free Cs3Bi2I9 perovskites for enhanced high-efficiency solar cells. Nanomaterials, 12(21), 3751.
2. Motsnyi, F. V., Vuychik, M. V., Smolanka, O. M., & Peresh, E. Y. (2005). Phase transition in $Cs_3Bi_2I_9$ ferroelastic: investigation by Raman scattering technique.
3. Machulin, V. F., Motsnyi, F. V., Peresh, E. Y., Smolanka, O. M., & Svechnikov, G. S. (2004). Effect of temperature variation on shift and broadening of exciton band in $Cs_3Bi_2I_9$ layered crystals.
4. Šiljegović, M. V., Petrović, J., Sekulić, D., Skuban, F., & Lukić-Petrović, S. R. (2020). Impedance response and I–V characteristics of Bi6 (As2S3) 94 and Bi7 (As2S3) 93 at elevated temperature. Journal of Materials Science: Materials in Electronics, 31(17), 14730-14736.
5. Biplab, G., Sudip, C., Hao, W., Claude, G., Shuzhou, L., Subodh, M., & Nripan, M. (2017). Poor Photovoltaic Performance of Cs3Bi2I9: An Insight through First-Principles Calculations.
6. Ghosh, B., Chakraborty, S., Wei, H., Guet, C., Li, S., Mhaisalkar, S., & Mathews, N. (2017). Poor photovoltaic performance of Cs3Bi2I9: an insight through first-principles calculations. The journal of physical chemistry C, 121(32), 17062-17067.
7. Medeiros, R. L., Melo, D. M., Oliveira, Â. A., Macedo, H. P., Fabris, G. S., Sambrano, J. R., ... & Morgado Jr, E. (2024). Effects of K, Rb, and Br doping on Cs3Bi2I9 perovskites: A design of experiments approach. Materials Science in Semiconductor Processing, 184, 108752.
8. Kang, J., Liu, J., Allen, O., Al-Mamun, M., Liu, P., Yin, H., ... & Zhao, H. (2022). Fabrication of High-Quality CsBi3I10 Films via a Gas-Assisted Approach for Efficient Lead-Free Perovskite Solar Cells. Energy Technology, 10(7), 2200318.
9. Li, W. G., Wang, X. D., Liao, J. F., Jiang, Y., & Kuang, D. B. (2020). Enhanced on–off ratio photodetectors based on lead-free Cs3Bi2I9 single crystal thin films. Advanced Functional Materials, 30(12), 1909701.
10. Bu, N., Jia, S., Xiao, Y., Li, H., Li, N., Liu, X., ... & Liu, S. F. (2022). Inch-size Cs 3 Bi 2 I 9 polycrystalline wafers with near-intrinsic properties for ultralow-detection-limit X-ray detection. Journal of Materials Chemistry C, 10(17), 6665-6672.
11. Li, X., Zhang, P., Hua, Y., Cui, F., Sun, X., Liu, L., ... & Tao, X. (2022). Ultralow detection limit and robust hard X-ray imaging detector based on inch-sized lead-free perovskite Cs3Bi2Br9 single crystals. ACS applied materials & interfaces, 14(7), 9340-9351.
12. Wei, S., Tie, S., Shen, K., Sun, H., Zheng, X., Wang, H., ... & Wu, J. (2022). Enhanced Carrier Transport in X-Ray Detector Based on Cs3Bi2I9/MXene Composite Wafers. Advanced Optical Materials, 10(23), 2201585.
13. Waykar, R., Bhorde, A., Nair, S., Pandharkar, S., Gabhale, B., Aher, R., ... & Jadkar, S. (2020). Environmentally stable lead-free cesium bismuth iodide (Cs3Bi2I9) perovskite: Synthesis to solar cell application. Journal of Physics and Chemistry of Solids, 146, 109608.
14. Zhang, H., Xu, Y., Sun, Q., Dong, J., Lu, Y., Zhang, B., & Jie, W. (2018). Lead free halide perovskite Cs 3 Bi 2 I 9 bulk crystals grown by a low temperature solution method. CrystEngComm, 20(34), 4935-4941.
15. Qi, Z., Fu, X., Yang, T., Li, D., Fan, P., Li, H., ... & Pan, A. (2019). Highly stable lead-free Cs3Bi2I9 perovskite nanoplates for photodetection applications. Nano Research, 12(8), 1894-1899.
16. Islam, M. T., Jani, M. R., Shorowordi, K. M., Hoque, Z., Gokcek, A. M., Vattipally, V., ... & Ahmed, S. (2021). Numerical simulation studies of Cs3Bi2I9 perovskite solar device with optimal selection of electron and hole transport layers. Optik, 231, 166417.
17. Zhang, J., Li, A., Li, B., Yang, M., Hao, X., Wu, L., ... & Zhang, J. (2022). Top-seed solution-based growth of perovskite Cs3Bi2I9 single crystal for high performance X-ray detection. ACS Photonics, 9(2), 641-651.